Complete transmission through a periodically perforated rigid slab

Lin Zhou[a)]
Department of Mathematical Sciences, University of Delaware, Newark, Delaware 19711

Gregory A. Kriegsmann
Department of Mathematical Sciences, New Jersey Institute of Technology, University Heights, Newark, New Jersey 07029

(Received 2 October 2006; revised 1 March 2007; accepted 5 March 2007)

The propagation of a normally incident plane acoustic wave through a three-dimensional rigid slab with periodically placed holes is modeled and analyzed. The spacing of the holes A and B, the wavelength λ, and the thickness of the slab L are order one parameters compared to the characteristic size D of the holes, which is a small quantity. Scattering matrix techniques are used to derive expressions for the transmission and reflection coefficients of the lowest mode. These expressions depend only on the transmission coefficient, τ_0, of an infinitely long slab with the same configuration. The determination of τ_0 requires the solution of an infinite set of algebraic equations. These equations are approximately solved by exploiting the small parameter $D/\sqrt{AB}$. Remarkably, this structure is transparent at certain frequencies and opaque for all others. Such a structure may be useful in constructing narrow-band filters and resonators. © *2007 Acoustical Society of America.* [DOI: 10.1121/1.2721878]

PACS number(s): 43.20.El, 43.20.Mv, 43.20.Bi [RMW] Pages: 3288–3299

I. INTRODUCTION

The propagation of acoustic and elastic waves through periodic structures with different mechanical properties has received considerable study.[1–9] These phenomena are similar to the propagation of electromagnetic waves in photonic crystals. The existence of pass and stop bands is a common feature shared by all. These are observed both theoretically[1,3,7] and experimentally.[5,6,8,9] In electromagnetic applications these photonic structures are used to construct frequency selective filters. Similarly, their acoustic counterparts are used in constructing vibrationless environments,[4] building ultrasonic transducers and filters, and designing new acousto-optical devices.[9]

In this paper, the propagation of acoustic waves is investigated for a particular periodic structure. It is a rigid slab with periodically perforated holes. The motivation for this research partly comes from the analogy between the periodic elastic composites and periodic dielectrics. Recently considerable attention has been focused on the propagation of electromagnetic waves through a particular two-dimensional, metallic grating.[10–12] This grating is a perfectly conducting metallic slab of finite thickness in which slits are periodically cut through it. It was found that at certain frequencies there is complete electromagnetic transmission through the structure although the width of the slits is much smaller than the incident wavelength and the spatial period of the structure. Several explanations of this phenomenon are given.[13,14] The acoustic analog of this problem consists of a rigid material, which plays the role of the metal slab, and an incident plane, acoustic wave, which takes the role of a properly polarized electromagnetic wave. Since the two-dimensional electromagnetic and acoustic problems are mathematically equivalent, the phenomenon will be the same. This is true when the grating is composed of a periodic array of closely space hard cylinders.[15] The purpose of this paper is to show that our three-dimensional structure has the same feature of complete transmission at certain discrete frequencies.

Our structure has been studied[16] for a slab of infinite length, with circular holes; it was used as a model of a simple porous medium. Reflection coefficients over a wide range of frequencies were investigated in detail to the first cutoff frequency by using perturbation analyses.

In this paper, we apply a scattering matrix technique to theoretically find the acoustic transmission properties of a rigid slab with periodically arranged air holes. Specifically, the scattering matrix of the structure is derived for arbitrarily shaped holes. It is found that this matrix depends on only one parameter. Under the assumption that the incident wavelength is of the same order as the spacing of the holes and is much bigger than the hole size, the total transmission and total reflection properties of the structure at certain frequencies are obtained for circular holes. In constructing the scattering matrices to show this interesting phenomena we revisit the problem considered in Ref. 16 and re-derive some of the results contained therein. However, the derivations in this paper are more straightforward and the results are obtained for general hole shapes. In this paper we show that our periodic structure possesses very sharp pass bands and very broad stop bands. That is, only certain discrete frequencies pass through the slab. This feature may be exploited to build filters and Fabry Perot resonators, the latter being constructed by placing two parallel slabs a few wavelengths apart.

[a)]Electronic mail: zhoulin@math.udel.edu

 0001-4966/2007/121(6)/3288/12/$23.00

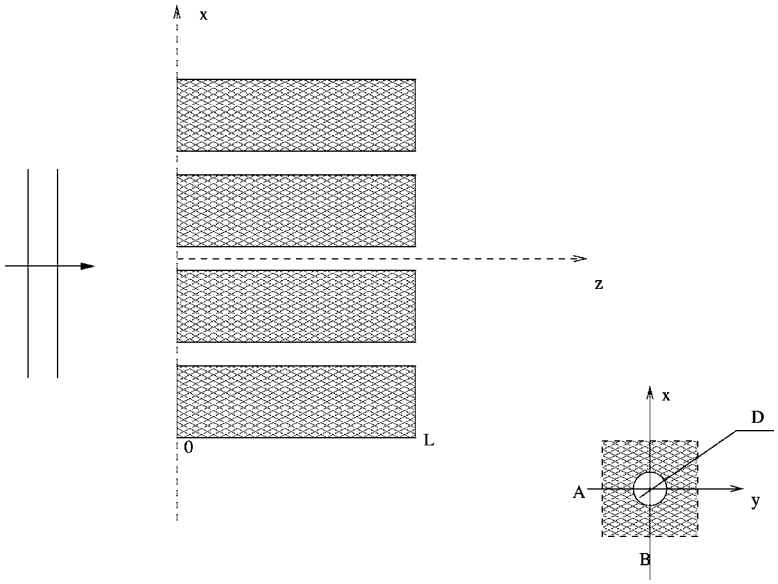

FIG. 1. Schematic diagram of the periodic structure considered in this problem.

The remainder of this paper is organized as follows. In Sec. II we present the mathematical formulation of the problem and our assumptions. This is followed by presenting modal solutions for each part of the structure. The form of the solution outside the slab is explicit. The solution inside the holes depends on their shape. However, the lowest eigenvalue and the eigenfunction for different shapes are found to be the same. In Sec. III we present and discuss two auxiliary problems, which are to construct the scattering matrix S for the structure. This allows both the transmission and the reflection coefficients to be obtained using S. We find remarkably that the transmission and reflection coefficients of our structure only depend upon one parameter, τ_0. This parameter is the transmission coefficient of the first auxiliary problem. In Sec. IV we present a Green's function argument in conjunction with a modal analysis to derive an infinite system of algebraic equations whose solution gives τ_0. In Sec. V, we exploit the small parameter D/S to obtain an approximation of τ_0 for the circular holes. In Sec. VI, we show that our structure possesses the complete transmission property described above. Finally, we present our conclusions in Sec. VII.

II. MATHEMATICAL FORMULATION

A schematic diagram of the structure is shown in Fig. 1. It is a rigid slab, infinitely long in both X and Y directions. In the Z direction the thickness of the slab is L. Holes are arranged periodically in the XY plane, and the cross section of the hole is uniform along the Z direction. All the holes are of the same shape. Since the structure is periodic, we consider a fundamental cell, which is also shown in Fig. 1. The length and the width of the fundamental cell are A and B, respectively. For an arbitrarily shaped hole, we define D, the square root of the hole's area, as the characteristic size of the hole.

A plane acoustic wave with frequency ω is normally incident on the perforated slab. The incident wavelength λ is of the same order as A and B. We assume that the viscosity of air is small enough so that the boundary layer on the surface of the hole channel can be neglected. Then the acoustic pressure U satisfies Helmholtz equation, $\nabla^2 U + K^2 U = 0$ both inside the pores and outside the slab. The constant K in the Helmholtz equation is the wave number defined by $K = 2\pi/\lambda$. The boundary condition is $\partial U/\partial n = 0$ on the rigid portions of the slab, where n denotes the normal direction to the rigid surfaces.

We assume that the hole is small compared to the size of the fundamental cell, that is, $D \ll \sqrt{AB}$. Under this assumption, it is intuitive that most of the incident wave will be reflected from the slab and only a small remnant of the wave will be able to reach the region $Z > L$. However, as mentioned above, we shall show that complete transmission is achieved at certain frequencies and slab thicknesses.

All upper case letters used so far represent dimensional parameters and variables. We will use lower case letters to denote the corresponding dimensionless quantities. We scale all lengths by $\sqrt{AB}$. Therefore, the fundamental cell has length a and width b, and $ab = 1$. The slab thickness $l = L/\sqrt{AB}$ and the dimensionless wave number $k = K\sqrt{AB}$ are both order one parameters in our problem. The dimensionless size of the hole is $d = D/\sqrt{AB} \ll 1$ by our assumption that $D \ll \sqrt{AB}$. The pressure U is scaled by the amplitude of the incident wave. After nondimensionalization, the governing equation and the boundary conditions become

$$\nabla^2 u + k^2 u = 0,$$
$$\frac{\partial u}{\partial n} = 0. \tag{1}$$

Since the structure is periodic and the incident wave strikes it normally, it is expected that in regions $z < 0$ and $z > l$, both u and its normal derivative are periodic functions of x and y with period a and b, respectively. By applying the boundary conditions, the solutions in regions $z < 0$ and $z > l$ can be written as eigenfunction expansions,

$$u(x,y,z) = e^{ikz}\psi_{00} + \sum_{m=0}^{\infty}\sum_{n=0}^{\infty} R_{mn}\psi_{mn}(x,y)e^{-i\beta_{mn}z}, \quad z < 0, \tag{2a}$$

$$u(x,y,z) = \sum_{m=0}^{\infty}\sum_{n=0}^{\infty} T_{mn}\psi_{mn}(x,y)e^{i\beta_{mn}z}, \quad z > l, \tag{2b}$$

where we have suppressed a time dependence of $e^{-i\omega t}$. In the region $z<0$, the solution consists of the incident wave $u_i = e^{ikz}$ and reflected waves. The unknowns R_{mn} are the amplitudes of the mnth reflected modes and β_{mn} are the corresponding propagation constants. In the region $z>l$, the mnth mode of the transmitted wave has an unknown amplitude T_{mn}. In (2a) and (2b) ψ_{mn} are normalized eigenfunctions of the periodic structure. If we choose the origin of the coordinate system to be at the center of the fundamental cell, these eigenfunctions can be written explicitly as

$$\psi_{00} = 1, \tag{3a}$$

$$\psi_{0n} = \sqrt{2}\cos\frac{2n\pi y}{b}, \quad \psi_{m0} = \sqrt{2}\cos\frac{2m\pi x}{a}, \tag{3b}$$

$$\psi_{mn} = 2\cos\frac{2m\pi x}{a}\cos\frac{2n\pi y}{b}, \quad m,n = 1,2,3,\ldots, \tag{3c}$$

and the propagation constants are

$$\beta_{mn} = \sqrt{k^2 - \frac{4m^2\pi^2}{a^2} - \frac{4n^2\pi^2}{b^2}}, \quad m,n = 0,1,2,\ldots. \tag{4}$$

In the channel where $0<z<l$, there are waves in both z and $-z$ directions. If we can find the eigenvalues and eigenfunctions corresponding to a particular hole shape, we can write down the solution of the Helmholtz equation in terms of the eigenvalues and eigenfunctions in this region, just as we did for the regions outside the slab. We know that for the Laplace operator with a Neumann boundary condition, all the eigenvalues are real and positive, therefore the eigenvalues can be ordered. Let λ_p denote the eigenvalues and φ_p denote the corresponding eigenfunctions, where $p = 0,1,2,\ldots$. Then the solution in the channel can be expressed as

$$u(x,y,z) = \sum_{p=0}^{\infty}(A_p e^{-ik_p z} + B_p e^{ik_p z})\varphi_p(x,y), \quad 0 < z < l. \tag{5}$$

In Eq. (5) the propagation constants k_p are defined as $k_p = \sqrt{k^2-\lambda_p^2}$, and the amplitudes A_p and B_p of each mode are unknown. Although the eigenvalues and eigenfunctions depend on the shape of the hole, the smallest eigenvalue and its corresponding normalized eigenfunction are the same for all shapes. The smallest eigenvalue is $\lambda_0 = 0$ and its corresponding eigenfunction is $\varphi_0 = 1/d$. Therefore, we have

$$k_0 = k, \tag{6a}$$

$$\varphi_0 = \frac{l}{d}. \tag{6b}$$

All the eigenvalues λ_p for $p \geq 1$ are greater than 0 and of order $1/d$. (The proof is given in Appendix A.) Since $\lambda_p \gg 1$, $k_p = i\sqrt{\lambda_p^2 - k^2}$ for any fixed k as $d \to 0$. Therefore, the propagation constants k_p can be approximated by

FIG. 2. A typical component of microwave circuits.

$$k_p \approx i\tilde{\lambda}_p/d, \quad p = 1,2,\ldots, \tag{7}$$

with $\tilde{\lambda}_p$ being order one quantities. This means that all the higher modes in the hole channel are highly damped.

III. THE METHOD

A. Scattering matrix method

In Sec. II, we derived solutions of the slab problem in terms of eigenfunction expansions. By finding the unknown coefficients of each mode, the problem will be solved completely. One way to find the unknown coefficients is by using the boundary conditions that connect the three regions, $z<0$, $0<z<l$, and $z>l$. This can be attained by using Green's function arguments to derive two integral equations, one at $z=0$ and the other at $z=l$, and substituting these modal solutions in the integral equations. Then, by exploiting the orthonormal properties of eigenfunctions, two coupled infinite systems of algebraic equations can be derived and solved numerically to obtain the transmission coefficients T_{mn} and the reflection coefficients R_{mn}.

The other approach to solve the problem is by the application of scattering matrix theory. In microwave circuit analysis and design, the scattering matrix is widely used to characterize a component, such as an amplifier or other circuit elements.[17] As shown in Fig. 2, a two-port circuit has two input voltages, a_0 and b_0, and two output voltages, c_0 and d_0. These are proportional to the strengths of the incident and reflected modes, respectively. They are connected through the scattering matrix S, which is often obtained experimentally, that is, the inputs and the outputs are related by the following equation,

$$\begin{bmatrix} c_0 \\ d_0 \end{bmatrix} = \begin{bmatrix} S_{11} & S_{12} \\ S_{21} & S_{22} \end{bmatrix}\begin{bmatrix} a_0 \\ b_0 \end{bmatrix} = S\begin{bmatrix} a_0 \\ b_0 \end{bmatrix}. \tag{8}$$

Once the scattering matrix S of the device is known and a_0 and b_0 are prescribed, the scattered amplitudes c_0 and d_0 are found from (8).

We are going to construct a scattering matrix for the slab problem, which connects the lowest mode of transmitted and reflected waves to the amplitudes of the incident waves. In order to do so, we will divide the slab into two parts at $z = l/2$. A scattering matrix for each part will be constructed individually. Then, neglecting the evanescent modes at $z = l/2$, a very good approximation by Eq. (7), we can combine these two matrices to construct S for our slab structure.

As a consequence of neglecting the exponentially small evanescent modes the acoustic field in the channel near $z = l/2$ is given by

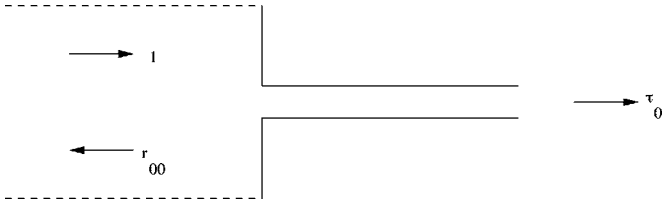

FIG. 3. Schematic diagram illustrating the structure and the incident, reflected, and transmitted waves considered in the first auxiliary problem.

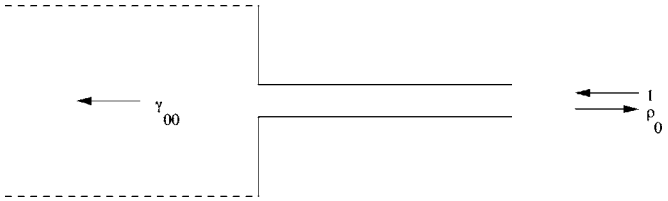

FIG. 4. Schematic diagram illustrating the structure and the incident, reflected, and transmitted waves considered in the second auxiliary problem.

$$u = (A_0 e^{-ikz} + B_0 e^{ikz})\varphi_0. \tag{9}$$

We now assume that $k<2\pi/a$ if $a>b$, otherwise $k<2\pi/b$. Then from Eq. (4) it follows that all the β_{mn} are purely imaginary except for β_{00}, which is equal to k. Thus, at a distance several wavelengths to the left of the aperture $z=0$, the field is

$$u = (e^{ikz} + R_{00} e^{-ikz})\psi_{00}. \tag{10}$$

Similarly, the transmitted acoustic field in the region $z>l$ is given by

$$u = T_{00} e^{ikz}\psi_{00}. \tag{11}$$

As we shall soon demonstrate, there exists a scattering matrix S_1 that connects the amplitudes of the outgoing waves R_{00} and. B_0 with the amplitudes of the incident waves 1 and A_0. The scattering matrix S_1 can be considered to characterize the first half of the structure $(-\infty<z<l/2)$.

We shall also show that there exists another scattering matrix S_2 that characterizes the second half of the structure $(l/2<z<\infty)$ and connects A_0, B_0, and T_{00}. A combination of the two scattering matrices S_1 and S_2 yields the scattering matrix S of the slab.

B. Two auxiliary problems

In order to determine matrices S_1 and S_2, we consider two auxiliary problems. The structure of these two auxiliary problems is the same as that of the fundamental cell, except that the channel is infinitely long $(l=\infty)$. This is the structure studied in Ref. 16.

In the first auxiliary problem, the wave is incident upon the periodic structure and is transmitted into the channel, as shown in Fig. 3. As before, we can write a modal solution of the problem as follows,

$$u(x,y,z) = e^{ikz}\psi_{00} + \sum_{m=0}^{\infty}\sum_{n=0}^{\infty} r_{mn}\psi_{mn}(x,y)e^{-i\beta_{mn}z}, \quad z<0, \tag{12a}$$

$$u(x,y,z) = \sum_{p=0}^{\infty} \tau_p \varphi_p(x,y)e^{ik_p z}, \quad z>0, \tag{12b}$$

in which u_1 denotes the acoustic pressure in the first auxiliary problem. The first transmission coefficient τ_0 and the first reflection coefficient r_{00} in Eqs. (12) are related by the simple equation

$$1 - r_{00} = d\tau_0. \tag{13}$$

Equation (13) is derived in the following way. To the left of $z=0$ (at $z=-\delta$), we differentiate u_1 with respect to z, then multiply $\partial u_1/\partial z$ by ψ_{00}. After integrating it over the area of the fundamental cell and using the orthonormality of the eigenfunctions, we obtain

$$\int_{-a/2}^{a/2}\int_{-b/2}^{b/2}\left(\left.\frac{\partial u_1}{\partial z}\right|_{z=-\delta}\right)\psi_{00}\,dx\,dy = ike^{-ik\delta} - ikr_{00}e^{ik\delta}. \tag{14}$$

Similarly, to the right of $z=0$ (at $z=\delta$) we have

$$\int\int_H \left(\left.\frac{\partial u_1}{\partial z}\right|_{z=\delta}\right)\varphi_0\,dx\,dy = ik\tau_0 e^{ik\delta}, \tag{15}$$

in which the double integral $\int\int_H$ is over the area of the hole. Letting $\delta\to 0$, the region of integration in (14) will coincide with H because $\partial u_1/\partial z=0$ outside the hole. Equation (13) now follows from the facts that $\partial u_1/\partial z$ is continuous in the hole at $z=0$ and $\varphi_0 d=\psi_{00}$.

The second auxiliary problem has the same structure as the first one. However, the wave is incident from the channel and is transmitted into the air region, as shown in Fig. 4. Therefore, the modal solution to this problem is

$$u_2(x,y,z) = \sum_{m=0}^{\infty}\sum_{n=0}^{\infty} \gamma_{mn}\psi_{mn}(x,y)e^{-i\beta_{mn}z}, \quad z<0, \tag{16a}$$

$$u_2(x,y,z) = e^{-ikz}\varphi_0 + \sum_{p=0}^{\infty} \rho_p \varphi_p(x,y)e^{ik_p z}, \quad z>0. \tag{16b}$$

Using the same argument as in the derivation of Eq. (13), it follows that the first transmission coefficient γ_{00} and the first reflection coefficient ρ_0 in the second auxiliary problem are related by

$$\gamma_{00} = d(1-\rho_0). \tag{17}$$

The two auxiliary problems are not independent. In Appendix B we prove that

$$\gamma_{00} = \tau_0. \tag{18}$$

Equations (13), (17), and (18) form a system of three equations in four unknowns. Thereby, we are able to express any three parameters in terms of the fourth. We choose to express γ_{00}, r_{00}, and ρ_0 in.terms of τ_0. Explicitly we have

$$r_{00} = 1 - d\tau_0, \tag{19a}$$

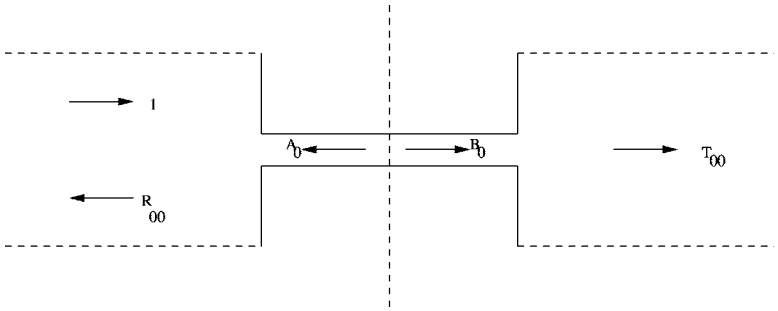

FIG. 5. Schematic diagram illustrating the structure and the incident, reflected, and transmitted waves considered in the slab structure.

$$\rho_0 = 1 - \frac{\tau_0}{d}, \tag{19b}$$

$$\gamma_{00} = \tau_0. \tag{19c}$$

The above result that any three of the four fundamental reflection and transmission coefficients can be written in terms of the fourth coefficient is also derived in Ref. 16, in which, a more complicated integral representation method is involved with the results holding only for circular holes.

These two auxiliary problems and their simple results enable us to find the scattering matrix of the slab, which depends on only one parameter.

C. Scattering matrix of the slab structure

Now we consider the slab problem. The scattering matrix for the first half $(-\infty < z < l/2)$ is derived by linearly combining the two auxiliary problems, since both the Helmholtz equation and the boundary conditions are linear. From Fig. 5 we observe that the first half of the structure can be viewed as having incident modes with amplitudes 1 and A_0, and reflected modes with amplitudes R_{00} and B_0. Hence, the results of the two auxiliary problems imply that

$$R_{00} = r_{00} \cdot 1 + \gamma_{00} A_0, \tag{20a}$$

$$B_0 = \tau_0 \cdot 1 + \rho_0 A_0. \tag{20b}$$

Rewriting Eq. (20) in matrix notation and using the relations given in Eq. (19) gives

$$\begin{bmatrix} R_{00} \\ B_0 \end{bmatrix} = S_1 \begin{bmatrix} 1 \\ A_0 \end{bmatrix}, \tag{21}$$

where the scattering matrix S_1 is

$$S_1 = \begin{bmatrix} 1 - d\tau_0 & \tau_0 \\ \tau_0 & 1 - \tau_0/d \end{bmatrix}. \tag{22}$$

The scattering matrix S_1 represents the first half of the slab structure. In Appendix C we prove that S_1 is unitary, i.e., $S_1 \bar{S}_1^T = I$, where T denotes the transpose of the matrix, the bar denotes the complex conjugate, and I is the 2×2 identity matrix. From this relationship it follows that

$$\left| \tau_0 - \frac{d}{1 + d^2} \right|^2 = \left(\frac{d}{1 + d^2} \right)^2. \tag{23}$$

The locus of Eq. (23) is a circle in the complex τ_0 plane. This circle can be equivalently expressed by

$$\tau_0 = \frac{2d}{1 + d^2 + i\eta}, \tag{24}$$

where $-\infty < \eta < \infty$, which is just a conformal mapping of the real line onto the circle.

We now derive the scattering matrix S_2, which relates the amplitudes of incident and reflected modes at the channel opening $z = l$. We introduce a new independent variable $\bar{z} = l - z$, which maps the second half of the structure into the first half. Using the result of S_1, we deduce that

$$S_2 = \begin{bmatrix} (1 - d\tau_0) e^{-2ikl} & \tau_0 \\ \tau_0 & (1 - \tau_0/d) e^{2ikl} \end{bmatrix}, \tag{25}$$

where e^{2ikl} and e^{-2ikl} take into account the physical location of the channel at $z = l$. Therefore, the amplitudes of outgoing waves T_{00} and A_0 are related to the amplitudes of the incoming waves B_0 by S_2, as follows,

$$\begin{bmatrix} T_{00} \\ A_0 \end{bmatrix} = S_2 \begin{bmatrix} 0 \\ B_0 \end{bmatrix} \tag{26}$$

One of the input wave amplitudes is 0 because there is no incident wave in the region $z > l$.

To determine a scattering matrix of our perforated slab structure, we first solve for A_0 in terms of B_0 from Eq. (21). Then we substitute A_0 in Eq. (26) and find B_0. The transmission coefficient T_{00} and the reflection coefficient R_{00} are determined from (21) and (26), respectively. These results are summarized as

$$\begin{bmatrix} R_{00} \\ T_{00} \end{bmatrix} = S \begin{bmatrix} 1 \\ 0 \end{bmatrix}, \tag{27}$$

where

$$S = \begin{bmatrix} (1 - d\tau_0) + \dfrac{\tau_0^2 (1 - \tau_0/d) e^{2ikl}}{M} & \dfrac{\tau_0^2}{M} \\ \dfrac{\tau_0^2}{M} & (1 - d\tau_0) e^{2ikl} + \dfrac{\tau_0^2 (1 - \tau_0/d)}{M} \end{bmatrix}, \tag{28}$$

and $M = 1 - (1 - \tau_0/d)^2 e^{2ikl}$. The scattering matrix S connects the reflected and transmitted waves of the lowest mode to the incident wave, as long as k is restricted to ensure single mode propagation in the regions $z < 0$ and $z > l$. It is important to note that S only depends on τ_0, which, from (24), is completely specified by η. Therefore, the reflection and transmission coefficients, R_{00} and T_{00}, only depend upon this one real parameter. This feature arises in the two-dimensional grating analyzed in Ref. 14. In the following

sections, we will approximate η numerically and find the transmission properties of the slab structure.

IV. THE DETERMINATION OF τ_0

The diagram of the first auxiliary problem is shown in Fig. 3. A part of the normally incident wave is reflected from this structure and the rest is transmitted into the channel. The modal solution, Eq. (12), of this problem was presented in Sec. III B, where the reflection and transmission coefficients are unknown. We shall now derive an expression for the field u_1 in the region $z<0$ using a standard Green's function representation. From this result we will deduce an infinite system of algebraic equations for the τ_n from which τ_0 will be determined.

The Green's function we employ satisfies

$$\nabla^2 G + k^2 G = \delta(\boldsymbol{x}-\boldsymbol{x}'), \quad z'<0, \tag{29a}$$

$$\frac{\partial G}{\partial z} = 0, \quad z=0, \tag{29b}$$

which is periodic in both x and y directions and represents outgoing, or evanescent, modes as $z\to\pm\infty$. It is explicitly given by

$$G(\vec{x}|\vec{x}') = \begin{cases} \displaystyle\sum_{-\infty}^{\infty}\sum_{-\infty}^{\infty} \frac{\cos\beta_{mn}z'}{i\beta_{mn}} e^{2m\pi i(x-x')/a} e^{2n\pi i(y-y')/b} e^{-ikz}, & -\infty < z < z', \\ \displaystyle\sum_{-\infty}^{\infty}\sum_{-\infty}^{\infty} \frac{\cos\beta_{mn}z}{i\beta_{mn}} e^{2m\pi i(x-x')/a} e^{2n\pi i(y-y')/b} e^{-ikz'}, & z' < z < 0. \end{cases} \tag{30}$$

Applying standard Green's function arguments, using the periodicity of both u_1 and G, their behaviors at infinity, and boundary conditions at $z=0$, we find that

$$u_1(x,y,z) = (2\cos kz)\psi_{00} - \int\int_H G(x',y',0^-|x,y,z)\frac{\partial u_1}{\partial z}(x',y',0^-)\,ds'. \tag{31}$$

Equation (31) is our integral representation of u_1 in the region $z<0$. The first term in Eq. (31) is the sum of the normally incident wave e^{ikz} and its rigid reflection e^{-ikz}. It is the field that would occur if no holes were present. In the second term, the integration is over the surface of the hole. Since the hole is small, the second term can be considered as a perturbation to the field in the region $z<0$ due to the existence of small holes in the structure.

Setting $z=0^-$ in Eq. (31), we obtain the field at the interface $z=0$,

$$u_1(x,y,0^-) = 2\psi_{00} - \int\int_H G(x',y',0^-|x,y,0^-) \times \frac{\partial u_1}{\partial z}(x',y',0^-)\,dx'\,dy'. \tag{32}$$

Since both u_1 and $\partial u_1/\partial z$ are continuous across $z=0$ on the surface of the hole, we let $z=0^+$ and substitute the modal expansion (12b) to obtain

$$\sum_{p=0}^{\infty}\tau_p\varphi_p(x,y) = 2\psi_{00} - \int\int_H G(x',y',0|x,y,0) \times \sum_{p=0}^{\infty} ik_p\tau_p\varphi_p(x',y')\,dx'\,dy'. \tag{33}$$

Multiplying both sides of this equation by φ_q, integrating the resulting equation over the surface of the hole, and using the othonormality of the eigenfunctions yields

$$\tau_q = 2d\delta_{q0} - i\sum_{p=0}^{\infty} k_p\tau_p Z_{qp}, \quad q=0,1,2,\ldots, \tag{34}$$

where

$$Z_{qp} = \int\int_H\int\int_H G(x',y',0|x,y,0)\varphi_p(x',y') \times \varphi_q(x,y)\,dx'\,dx\,dy'\,dy \tag{35}$$

and δ_{q0} is the Kronecker delta function. We recall from Eq. (7) and our limit $d\to 0$ that $k_p = i|k_p|$ for $p\geq 1$. Using this observation we rewrite Eq. (34) as

$$\tau_0 = 2d - ik\tau_0 Z_{00} + \sum_{p=1}^{\infty}|k_p|Z_{0p}\tau_p, \tag{36a}$$

$$\tau_q = ik\tau_0 Z_{q0} + \sum_{p=1}^{\infty}|k_p|Z_{qp}\tau_p, \quad q=1,2,\ldots. \tag{36b}$$

The equations in (36) form an infinite system of algebraic equations with unknowns τ_p. The quantities Z_{qp} are defined in (35). If the eigenfunctions φ_p are known, Z_{qp} can be found either analytically or numerically for each p and q. There-

fore, each τ_p can be solved for approximately by truncating the infinite system.

Before truncating the algebraic system (36), we simplify it further, so as to find an explicit representation for τ_0 that is comparable to (24). Setting $\alpha_q=\tau_q/(-ik\tau_0)$ for $q\geq 1$ and substituting α_q in (36b) gives

$$\alpha_q = Z_{q0} + \sum_{p=1}^{\infty} |k_p| Z_{qp}\alpha_p, \quad q = 1,2, \ldots . \tag{37}$$

The same change of variable applied to (36a) yields

$$\tau_0 = \frac{2d}{1 + ikZ_{00} + ik\sum_{p=1}^{\infty} |k_p| Z_{0p}\alpha_p}. \tag{38}$$

Thus, τ_0 can be found explicitly provided that Eq. (37) can be solved for the α_q.

The quantities Z_{qp} depend upon the shape of the hole. However, the first eigenfunction $\varphi_0=1/d$ is the same for all shapes. Therefore, we deduce from Eq. (35) that Z_{00} is given by

$$Z_{00} = \int \int_H \int \int_H G(x',y',0|x,y,0)\frac{1}{d^2}\, dx'\, dx\, dy'\, dy. \tag{39}$$

Now, G in Eq. (30) can be rewritten for $z=z'=0$ as

$$\begin{aligned} G(x',y',0|x,y,0) = {} & \frac{1}{ik} - \sum_{n=1}^{\infty} \frac{2}{|\beta_{0n}|} \cos\frac{2n\pi(y-y')}{b} \\ & - \sum_{m=1}^{\infty} \frac{2}{|\beta_{m0}|} \cos\frac{2m\pi(x-x')}{a} \\ & - \sum_{m=1}^{\infty}\sum_{n=1}^{\infty} \frac{4}{|\beta_{mn}|} \cos\frac{2m\pi(x-x')}{a} \\ & \times \cos\frac{2n\pi(y-y')}{b}, \end{aligned} \tag{40}$$

where we have used that fact that $\beta_{nm}=i|\beta_{nm}|$ for our restricted values of k. Substituting this into the expression for Z_{00} and integrating the first term implies that the first term is d^2/ik for any shape of the hole. Hence, Z_{00} can be rewritten as

$$Z_{00} = \frac{d^2}{ik} + \tilde{Z}_{00}, \tag{41}$$

where $\tilde{Z}_{00}$ is real. Finally, substituting this result into Eq. (38) gives

$$\tau_0 = \frac{2d}{1 + d^2 + ik(\tilde{Z}_{00} + \sum_{p=1}^{\infty} |k_p| Z_{0p}\alpha_p)}. \tag{42}$$

Equations (42) and (24) are identical with

$$\eta = k\left(\tilde{Z}_{00} + \sum_{p=1}^{\infty} |k_p| Z_{0p}\alpha_p\right). \tag{43}$$

Thus, τ_0 lies on the circle given by Eq. (23) regardless of the shape of the hole. We observe that the system (37) must be truncated in order to obtain an approximate solution for the α_q. Once these are determined, then Eqs. (42) and (43) can be truncated to yield an approximation to τ_0, and this in turn will be used to approximate T_{00}. It is interesting to note in closing this section that our truncated approximation of τ_0 satisfies (24) regardless of either the truncation level or the accuracy used in computing the Z_{qp}. However, the accurate location of τ_0 on this circle requires careful approximations and truncations.

V. AN APPROXIMATION TO τ_0 FOR CIRCULAR HOLES

In the expression for τ_0 in Eq. (42), the real number η needs to be computed. Since η is a function of Z_{qp} and α_q [Eq. (43)], we shall first evaluate the parameters Z_{qp} and α_q in order to determine η and hence determine τ_0. In this section, τ_0 is determined for circular holes.

If the dimensional radius of the hole is R, then the characteristic size of the hole is $D=\sqrt{\pi}R$. After nondimensionalization, we obtain that $d=\sqrt{\pi}r$. Therefore, the eigenfunctions corresponding to the circular hole can be easily obtained as follows,

$$\varphi_0 = \frac{1}{d}, \tag{44}$$

$$\varphi_p(r) = \frac{1}{d}\frac{J_0(\lambda_p r)}{J_0(\lambda_p d/\sqrt{\pi})}, \quad p = 1,2, \ldots , \tag{45}$$

where J_0 is the zeroth order Bessel function. The corresponding eigenvalues are found to be $\lambda_p=j_{1p}\sqrt{\pi}/d$, where j_{1p} is the pth root of the first order Bessel function. Note that only the radial eigenfunctions are employed since the incident wave impinges normally upon the slab. As mentioned before, for $d\ll 1$, the propagation constants

$$k_p = \sqrt{k^2 - \lambda_p^2} \tag{46}$$

in the channel can be approximated by

$$k_p \approx ij_{1p}\sqrt{\pi}/d, \quad p \geq 1. \tag{47}$$

Now, the quantities Z_{qp} can be found explicitly using the explicit expressions of the Green's functions and the eigenfunctions. The integral in Eq. (35) is computed by interchanging the order of integration and the summation. The results of these calculations yield

$$\begin{aligned} Z_{00} = {} & \frac{d^2}{ik} + d^2\left(\sum_{m=1}^{\infty} \frac{-8}{|\beta_{m0}|}\frac{J_1^2(\mu_1)}{\mu_1^2} + \sum_{n=1}^{\infty} \frac{-8}{|\beta_{0n}|}\frac{J_1^2(\mu_2)}{\mu_2^2} \right. \\ & \left. + \sum_{m=1}^{\infty}\sum_{n=1}^{\infty} \frac{-16}{|\beta_{mn}|}\frac{J_1^2(\mu_3)}{\mu_3^2}\right) \equiv \frac{d^2}{ik} + d^2 S_{00}, \end{aligned} \tag{48}$$

$$Z_{qp} = d^2 \sum_{m=1}^{\infty} \frac{-8}{|\beta_{m0}|} \frac{\mu_1^2 J_1^2(\mu_1)}{(\mu_1^2 - j_{1p}^2)(\mu_1^2 - j_{1q}^2)} + d^2 \sum_{n=1}^{\infty} \frac{-8}{|\beta_{0n}|} \frac{\mu_2^2 J_1^2(\mu_2)}{(\mu_2^2 - j_{1p}^2)(\mu_2^2 - j_{1q}^2)} + d^2 \sum_{m=1}^{\infty} \sum_{n=1}^{\infty} \frac{-16}{|\beta_{mn}|} \frac{\mu_3^2 J_1^2(\mu_3)}{(\mu_3^2 - j_{1p}^2)(\mu_3^2 - j_{1q}^2)} \equiv d^2 S_{qp},$$

$$p^2 + q^2 \geq 1, \tag{49}$$

where μ_1, μ_2, and μ_3 are defined as

$$\mu_1 = 2m\sqrt{\pi}d/a, \tag{50a}$$

$$\mu_2 = 2n\sqrt{\pi}d/b, \tag{50b}$$

$$\mu_3 = \sqrt{(2m\sqrt{\pi}d/a)^2 + (2n\sqrt{\pi}d/b)^2}. \tag{50c}$$

We observe that in Eq. (49), the quantities Z_{qp} are symmetric and hence $S_{pq}=S_{qp}$. Substituting the new notation in Eqs. (37) and (42), respectively, gives

$$\alpha_q = d^2 S_{q0} + d^2 \sum_{p=1}^{\infty} |k_p| S_{qp} \alpha_p, \quad q = 1,2, \ldots, \tag{51}$$

and

$$\tau_0 = \frac{2d}{1 + d^2 + id^2(kS_{00} + k\sum_{p=1}^{\infty} |k_p| S_{0p}\alpha_p)}. \tag{52}$$

The infinite system of equations (51) cannot be solved exactly; it must be truncated to obtain approximations to the α_q. For a fixed N we denote by $\hat{\alpha}_q$ the approximate solution of (51), which satisfies

$$\hat{\alpha}_q = d^2 S_{q0} + d \sum_{p=1}^{N} j_{1p}\sqrt{\pi} S_{qp} \hat{\alpha}_p, \tag{53}$$

where (47) has been used for simplification. The corresponding approximation to τ_0 is denoted by $\hat{\tau}_0$, which is obtained from (52) by truncating the series at $p=N$. We have solved (53) for values of d ranging from 0.01 to 0.1, for several values of N. We have found for these values of d that the corresponding values of $\hat{\tau}_0$ are accurate to four decimal places when $N=3$, i.e., increasing N does not significantly alter their values. These results are similar to the trends seen in the related problem of Ref. 14.

We will now derive an approximate solution of (53) and the corresponding approximation of $\hat{\tau}_0$ by exploting the smallness of d. Before doing this, we first check the order of S_{qp} as d approaches 0. Figures 6, 7, and 8 show this behavior for S_{00}, S_{0p}, and S_{qp}, respectively. In Fig. 6 we observe that, as d approaches 0, S_{00} increases and behaves like $1/2d$. In Figs. 7 and 8 we observe that the S_{0p} and S_{qp} are very small compared to S_{00}, and both the S_{0p} and S_{qp} are order one quantities as d approaches 0.

Using the fact that both the S_{0p} and S_{qp} are of $O(1)$ for small values of d and the fact that $d \ll 1$, a simple approximation to Eq. (53) yields

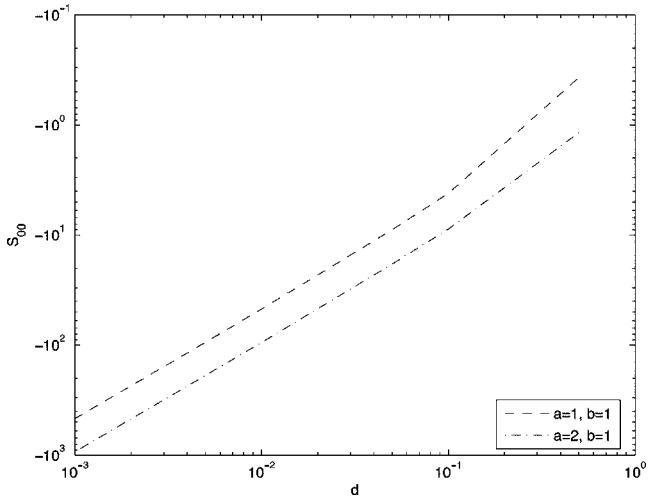

FIG. 6. The behavior of S_{00} for small values of d.

$$\hat{\alpha}_q = d^2 S_{q0} + O(d^3), \quad 1 \leq q \leq N. \tag{54}$$

Substituting this expression into the truncated version of Eq. (52) we obtain the approximation to $\hat{\tau}_0$:

$$\hat{\tau}_0 = \frac{2d}{1 + d^2 + ikd^2\{S_{00} + d^2 \sum_{p=1}^{N} j_{1p}\sqrt{\pi} S_{0p}^2\}}. \tag{55}$$

As d approaches 0, the second term in curly brackets is much smaller than the first term. This is because the S_{0p} are of $O(1)$ and S_{00} is of $O(1/d)$ for $d \ll 1$. Therefore, neglecting the second term in (55) we obtain

$$\hat{\tau}_0 = \frac{2d}{1 + d^2 + id^2 k S_{00}}. \tag{56}$$

This approximation satisfies the constraint (24) and, more importantly, is remarkably accurate. It agrees to within three decimal places of the numerical results obtained from solving (53) and the truncated version of (52).

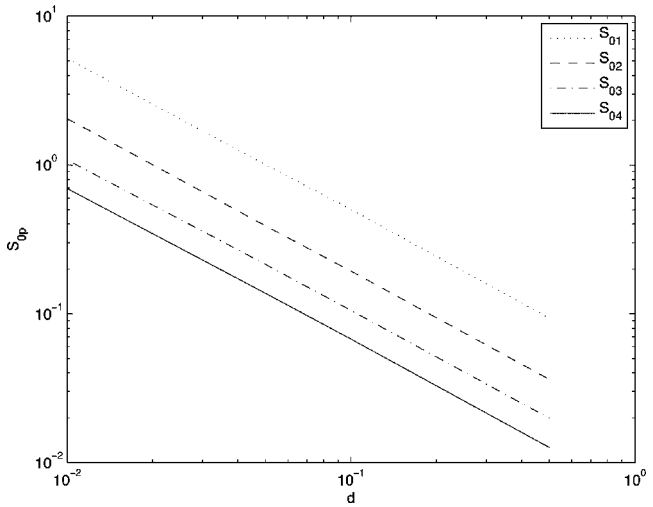

FIG. 7. The behavior of S_{0p} for small values of d.

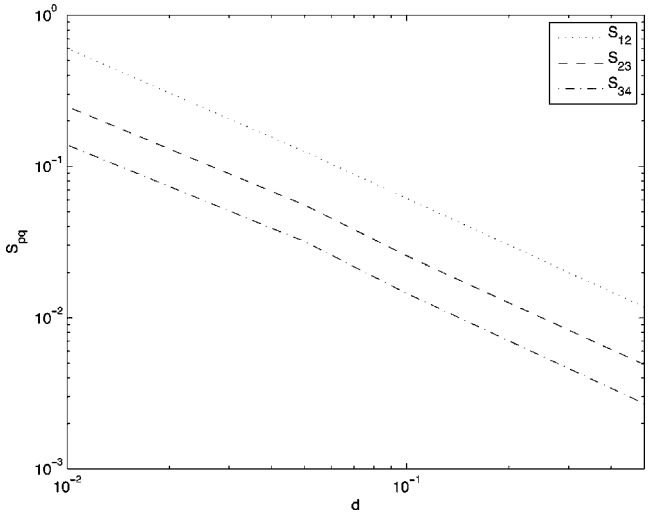

FIG. 8. The behavior of S_{qp} for small values of d.

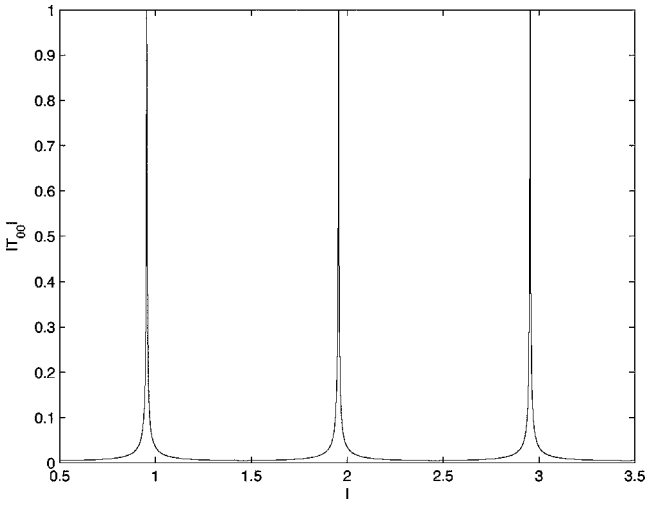

FIG. 9. Transmission coefficient T_{00} versus the thickness of the slab l for $d=0.05$, $k=\pi$, and $a=b=1$.

VI. TRANSMISSION PROPERTIES

Through the analysis in Sec. V, we obtained an approximation of τ_0 for small values of d. We are now ready to numerically approximate T_{00}. From Eqs. (27) and (28) we readily solve for T_{00} and find

$$T_{00} = \frac{\tau_0^2}{1-(1-\tau_0/d)^2 e^{2ikl}}. \tag{57}$$

Substituting the approximation $\hat{\tau}_0$ from Eq. (56), we find that

$$|\hat{T}_{00}| = \frac{2d^2}{\sqrt{(2d^2\nu_1)^2+\nu_2^2}},$$

$$\nu_1 = d^2 k S_{00} \sin kl + \cos kl, \tag{58}$$

$$\nu_2 = (1+d^4-d^4k^2S_{00}^2)\sin kl - 2d^2kS_{00}\cos kl.$$

We note here that the formula (58) for T_{00} can be obtained by carefully summing up the internal reflections within the slit using the reflection and transmission coefficients from the two auxiliary problems and their relationships to τ_0.

From this expression of the transmission coefficient, we observe that if kl is such that ν_2 is an order one quantity, then T_{00} is $O(d^2)$, which is very small and there is very little transmission into the region $z>l$. This agrees with our intuition, because when the holes are small, most of the acoustic wave reflects back into $z<0$. However, there exist values of kl such that $\nu_2=0$, that is,

$$\tan kl = \frac{2d^2kS_{00}}{1+d^4(1-k^2S_{00})}; \tag{59}$$

then, in this case,

$$|\hat{T}_{00}| = 1/\nu_1 = \frac{1/\cos kl}{1+d^2kS_{00}\tan kl}. \tag{60}$$

Using the fact that $d \ll 1$, the values of kl that approximately satisfy (59) are

$$kl \approx M\pi + 2d^2kS_{00} + O((d^2S_{00})^2), \tag{61}$$

where M is any positive integer. Using the these values of kl in Eq. (60), we deduce

$$|\hat{T}_{00}| \approx 1 - O((d^2S_{00})^4). \tag{62}$$

Therefore, for these values of kl, the slab is almost transparent. This transparency is caused by a resonance phenomenon in the small channels. Although only a small amount of the wave propagates into a channel, $\tau_0=O(1)$, it constructively reflects back and forth within. This reflection is almost perfect within the channel because $\rho_0=1-\tau_0/d\sim-1$. The leading order approximation of kl from (61), $kl\sim M\pi$, would occur if the channel openings were replaced by sound soft surfaces. Thus, the result given by (61) shows the channels behave as leaky resonators. The numerical results presented in the next two paragraphs support this interpretation.

The transmission coefficient given Eq. (58) is plotted in Fig. 9 as a function of l for $k=\pi$ and $d=0.05$. It shows that T_{00} is almost 0 for all thicknesses l of the slab except at $l \approx 1,2,3,\ldots$, where $T_{00}\approx 1$. Actually, the peaks occur just to the left of these integers. The difference agrees with our approximation for l. This agreement is also seen in Fig. 10, where $k=\pi$, $S_{00}=-4.33$, and $d=0.1$. In this figure, the peaks appear some distance to the left of $l=1,2,3,\ldots$, and the difference is 0.086, which equals $2d^2S_{00}$. Also, Figs. 9 and 10 verify that, away from the peaks, the values of T_{00} are $O(d^2)$. The resonances shown in these figures are very sharp due to the fact that there are no losses in our model. We can relax this idealization in a phenomenological way by making the wave number k slightly complex. The result is shown in Fig. 11 where the dashed curve corresponds to $\mathrm{Im}(k)=0.05$ and the solid to $\mathrm{Im}(k)=0.01$. In both cases $\mathrm{Re}(k)=\pi$ and $d=0.1$. It is clear that increasing the imaginary part of k diminishes the resonant peaks and effectively spreads out the response as a function of l.

Similarly, we can fix the thickness of the slab and solve Eq. (59) for k to find the frequency at which the structure is transparent. Since S_{00} is also a function of k, it is not easy to find an explicit expression. However, it is easy to check nu-

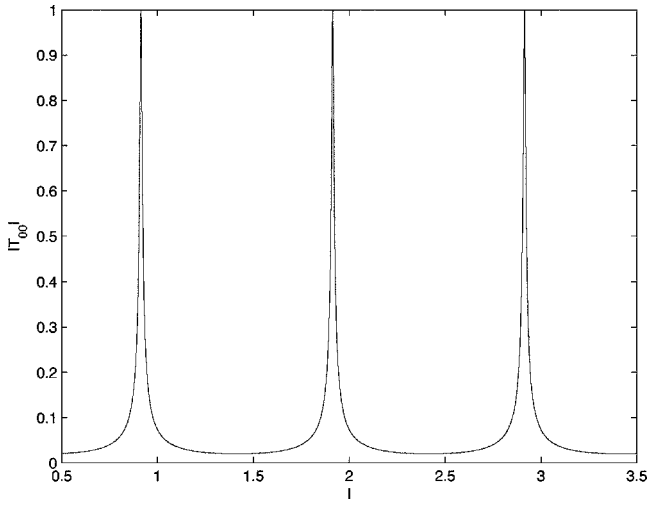

FIG. 10. Transmission coefficient T_{00} versus the thickness of the slab l for $d=0.1$, $k=\pi$, and $a=b=1$.

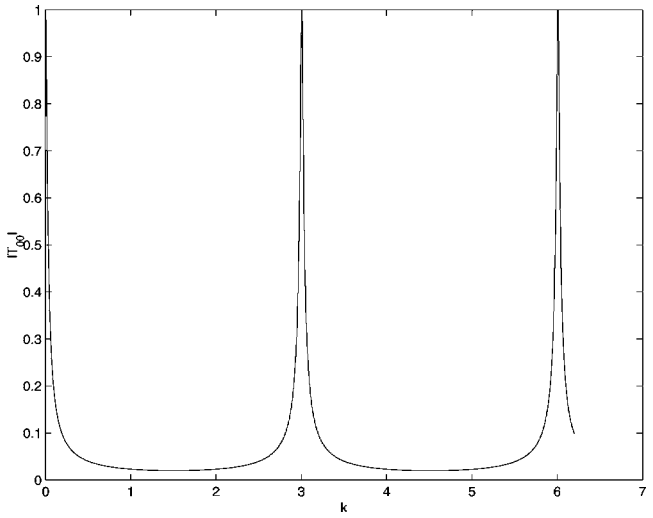

FIG. 12. Transmission coefficient T_{00} versus wave number k for $d=0.1$, $l=1$, and $a=b=1$.

merically that, when $k<2\pi/a$, S_{00} is not a sensitive function of k. Thus from Eq. (61), k can be approximated as

$$k \approx \frac{M\pi}{l - 2d^2 S_{00}}. \tag{63}$$

For these values of k, $T_{00} \approx 1$. The behaviors of $|T_{00}|$ as a function of k are illustrated in Figs. 12 and 13, where $l=1$ and 2, respectively. The peaks occur just at the position estimated by Eq. (63). The number of peaks increases as l increases when the upper limit of k is fixed. Again, the resonance shown in these figures is very sharp. These can be smoothed somewhat by taking into account a small amount of viscosity in the acoustic fluid. This amounts to letting the imaginary part of the wave number depend quadratically on frequency, or equivalently replacing k by $k+ik^2\epsilon$, where ϵ is a small number depending upon viscosity. The results for this case are shown in Fig. 14. The resonances become less pronounced as ϵ and the frequency are increased.

It is clear from these figures that the perforated rigid slab behaves like a narrow-band filter, in the absence of losses. For certain frequencies, energy is transmitted almost 100%; for other frequency bands, almost all the energy is reflected. Also, the widths of the pass bands depend on the dimensionless radius of the holes. If dimensions are reintroduced, then these widths would depend upon the porosity of the rigid slab. However, it is also clear from our figures that the practical use of this structure, as a filter, will be limited by the losses present in a real application.

Finally, we note that our results can be extended to noncircular channels. The calculations become complex, even in the case of square crossections. The reader is referred to Ref. 18 for the details of this case.

VII. CONCLUSION

In this paper, we have analyzed the transmission properties of a periodically perforated rigid slab under normal, plane wave incidence. We have assumed that the characteristic size of a hole is much smaller than the spacing of the holes, while the incident wave length is of the same order as

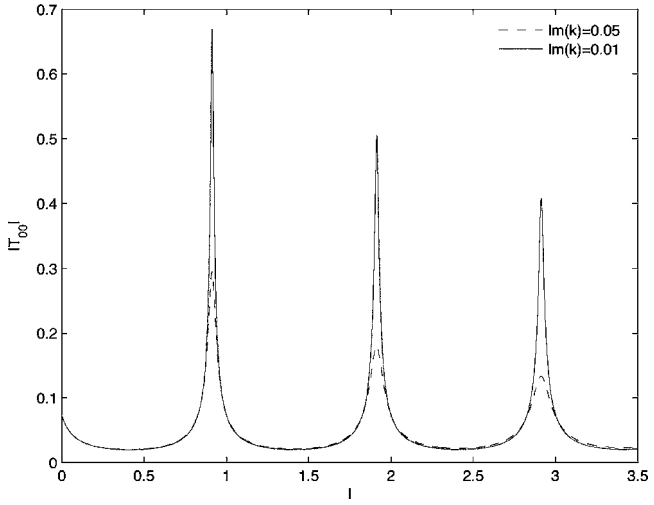

FIG. 11. Transmission coefficient T_{00} versus the thickness of the slab l for $d=0.1$, $\mathrm{Re}(k)=\pi$, and $a=b=1$.

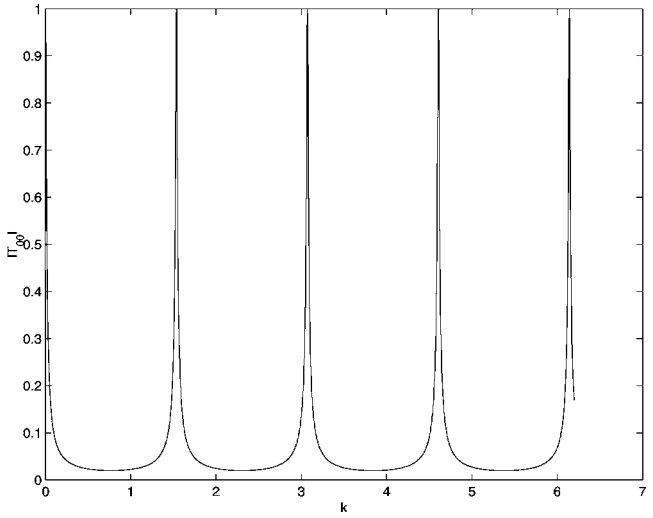

FIG. 13. Transmission coefficient T_{00} versus wavenumber k for $d=0.1$, $l=2$, and $a=b=1$.

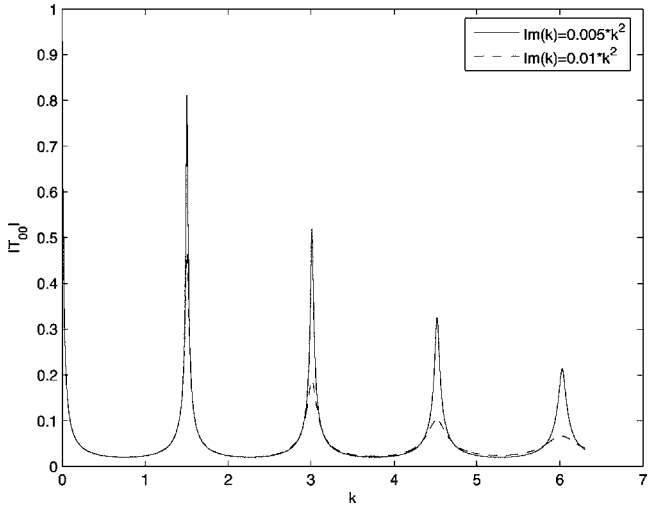

FIG. 14. Transmission coefficient T_{00} versus $Re(k)$ for $d=0.1$, $l=2$, and $a=b=1$.

the hole spacing. We have also restricted the range of the incident wave frequency such that only one mode propagates outside the slab and inside the holes. The length of the slab in our problem is long enough so that all the evanescent modes are negligible in the middle of the hole channel. Under these assumptions, we have considered two auxiliary problems. Both of the auxiliary problems have the same structure as the slab except that they are infinitely long. In the first auxiliary problem, the wave is incident from the air; in the second auxiliary problem, the wave is incident from the hole. The relationship of the transmission and the reflection coefficients of the two problems were discussed in detail. The linear combination of the two auxiliary problems gave a scattering matrix S for the original structure. Through this matrix, the transmission coefficient T_{00} and the reflection coefficient R_{00} of the slab were found explicitly. We have found that, for arbitrary shaped holes, the coefficients T_{00} and R_{00} depend only on one parameter τ_0, which is the transmission coefficient of the first auxiliary problem. This coefficient was found to lie on a circle in the complex plane.

Numerical values of τ_0 were found for circular holes. Specifically, an infinite system of algebraic equations was derived from the integral representation of the solution of the first auxiliary problem. The coefficient τ_0 was explicitly obtained from these algebraic equations. By using the fact that the hole size is very small compared to the spacing of the holes, τ_0 was obtained numerically. The plots of $|T_{00}|$ were given for circular holes. The plots showed that for fixed thickness of the slab, the function $|T_{00}|$ is $O(d^2)$ quantities except at certain frequencies, at which the wave can transmit almost completely. On the other hand, if the frequency of the incident wave is fixed, by adjusting the thickness of the slab, we can have either completely transmitted or a completely reflected wave. We have also considered the effects of losses on the resonant behavior of our structure. If these are not too large, then our structure may be potentially useful in constructing filters and resonators.

APPENDIX A

In this appendix we will find the order of eigenvalues of a general hole shape. The characteristic size of the hole is d, which is defined as the square root of the area of the hole. We assume that the eigenvalues and the eigenfunctions are λ_p and φ_p, respectively, with $p=0,1,2,\ldots$. They satisfy the following equation:

$$\nabla^2\varphi_p(x,y) = -\lambda_p^2\varphi_p(x,y). \tag{A1}$$

Let $x'=x/d$ and $y'=y/d$. Then x' and y' are $O(1)$ variables. After changing of variables, the eigenvalue problem becomes

$$\frac{\partial^2\varphi_p}{\partial x'^2} + \frac{\partial^2\varphi_p}{\partial y'^2} = -d^2\lambda_p^2\varphi_p, \tag{A2}$$

where the domain is independent of d and is thus $O(1)$. The eigenvalues for this problem are $\Lambda_p=d^2\lambda_p^2$ and these are $O(1)$ quantities, which depend upon the geometry of this scaled domain. Hence the $\lambda_p=O(1/d)$ as $d\to 0$.

APPENDIX B

To prove $\gamma_{00}=\tau_0$, we consider the equation

$$\nabla\cdot\{u_2\nabla u_1 - u_1\nabla u_2\} = 0. \tag{B1}$$

Integrating it over the cube $|z|<z_\infty$, $|x|<a/2$, $|y|<b/2$ and applying the divergence theorem, we obtain

$$\int\int\left(u_2\frac{\partial u_1}{\partial n} - u_1\frac{\partial u_2}{\partial n}\right)ds = 0, \tag{B2}$$

where the double integral is over the six surfaces of the cube and n is the normal direction of each surface. The integrals over four surfaces cancel off with each other because of the periodic boundary conditions. Therefore, only the surface integrals over the top and the bottom remain, which gives

$$\int_{-a/2}^{a/2}\int_{-b/2}^{b/2}\left(u_2\frac{\partial u_1}{\partial z} - u_1\frac{\partial u_2}{\partial z}\right)\Bigg|_{z=-\infty} dx\,dy = \int\int_H\left(u_2\frac{\partial u_1}{\partial z} - u_1\frac{\partial u_2}{\partial z}\right)\Bigg|_{z=\infty} dx\,dy. \tag{B3}$$

After substituting infinite series expansions for u_1 and u_1 in this equation, most terms cancel off. We obtain

$$2ik\gamma_{00} = 2ik\tau_0, \tag{B4}$$

which yields the result $\gamma_{00}=\tau_0$.

APPENDIX C

Suppose we chose k properly such that all the higher order modes are evanescent. Then, generally, we have $u_1=a_0e^{-ikz}+b_0e^{ikz}$ at $z=-\infty$ and $u_1=c_0e^{ikz}+d_0e^{-ikz}$ at $z=\infty$. Considering $\nabla\cdot\{\bar{u}_1\nabla u_1 - u_1\nabla\bar{u}_1\}=0$, which is equivalent to $\nabla\cdot\{\Im(\bar{u}_1\nabla u_1)\}=0$, by using the same procedure as was done in Appendix A, we obtain

$$\int_{-a/2}^{a/2}\int_{-b/2}^{b/2}\Im\left(\bar{u}_1\frac{\partial u_1}{\partial z}\right)\Bigg|_{z=-\infty} dx\,dy = \int\int_H\Im\left(\bar{u}_1\frac{\partial u_1}{\partial z}\right)\Bigg|_{z=\infty} dx\,dy. \tag{C1}$$

Substituting the expression of u_1 at $z=\pm\infty$ in Eq. (C1) yields

$$|a_0|^2 + |c_0|^2 = |b_0|^2 + |d_0|^2. \tag{C2}$$

We know that a_0, b_0, c_0, and d_0 are related by matrix S_1, that is,

$$b_0 = (1 - d\tau_0)a_0 + \tau_0 c_0, \tag{C3a}$$

$$d_0 = \tau_0 a_0 + (1 - \tau_0/d)c_0. \tag{C3b}$$

Inserting them into Eq. (C2) gives

$$\{|1 - d\tau_0|^2 + |\tau_0|^2 - 1\}|a_0|^2 + \{|1 - \tau_0/d|^2 + |\tau_0|^2 - 1\}|c_0|^2 + 2\Re\{(1 - d\bar{\tau}_0)\tau_0\bar{a}_0 c_0 + (1 - \tau_0/d)\bar{\tau}_0\bar{a}_0 c_0\} = 0. \tag{C4}$$

Setting $a_0=1$, $c_0=0$ and $a_0=0, c_0=1$, respectively, we have three equations

$$|1 - d\tau_0|^2 + |\tau_0|^2 = 1, \tag{C5a}$$

$$|1 - \tau_0/d|^2 + |\tau_0|^2 = 1, \tag{C5b}$$

$$\tau_0 + \bar{\tau}_0 - d|\tau_0|^2 - |\tau_0|^2/d = 0, \tag{C5c}$$

which proves that $S_1 \cdot \bar{S}_1^T = I$.

[1] M. Sigalas and E. Economou, "Band structure of elastic wave in two dimensional systems," Solid State Commun. **86**, 141–143 (1993).

[2] M. Kushwaha, P. Halevi, L. Dobrzynski, and B. Djafari-Rouhani, "Acoustic band structure of periodic elastic composites," Phys. Rev. Lett. **71**, 2022–2025 (1993).

[3] M. Kushwaha, P. Halevi, G. Martinez, L. Dobrzynski, and B. Djafari-Rouhani, "Theory of acoustic band structure of periodic elastic composite," Phys. Rev. B **49**, 2313–2322 (1994).

[4] M. Kushwaha, "Stop-band for periodic metallic rods: Sculptures that can filter the noise," Appl. Phys. Lett. **70**, 3218–3220 (1997).

[5] Z. Liu, X. Zhang, Y. Mao, Y. Zhu, Z. Yang, C. Chan, and P. Sheng, "Locally resonant sonic materials," Science **289**, 1734–1736 (2000).

[6] S. Yang, J. Page, Z. Liu, M. Cowan, C. Chan, and P. Sheng, "Ultrasound tunneling through 3D photonic crystals," Phys. Rev. Lett. **88**, 104301-1–104301-4 (2002).

[7] C. Goffaux and J. Sanchez-Dehesa, "Two-dimensional photonic crystals studies using a variational method: Application to lattices of locally resonant materials," Phys. Rev. B **67**, 144301 (2003).

[8] S. Zhang and J. Cheng, "Existence of broad acoustic band gaps in three-component composite," Phys. Rev. B **68**, 245101 (2003).

[9] T. Gorishnyy, C. Ullal, M. Maldovan, G. Fytas, and E. Thomas, "Hypersonic photonic crystals," Phys. Rev. Lett. **94**, 115501 (2005).

[10] T. W. Ebbesen, H. J. Lezek, H. F. Ghaemi, T. Thio, and P. A. Wolff, "Extraordinary optical transmission through sub-wavelength hole arrays," Nature (London) **391**, 667–669 (1998).

[11] A. P. Hibbins and J. R. Sambles, "Remarkable transmission of microwaves through a long wall of metallic bricks," Appl. Phys. Lett. **79**, 2844–2846 (2001).

[12] J. A. Porto, F. J. Garcia-Vidal, and J. B. Pendry, "Transmission resonances on metallic gratings with very narrow slits," Phys. Rev. Lett. **83**, 2845–2848 (1999).

[13] I. Anderson, "Comment on Remarkable transmission of microwaves through a wall of long metallic bricks," Appl. Phys. Lett. **82**, 308–309 (2003).

[14] G. A. Kriegsmann, "Complete transmission through a two-dimensional diffraction grating," **65**, 24–42 (2004).

[15] X. Zhang, "Acoustic resonant transmission through acoustic gratings with very narrow slits: Multiple-scattering numerical simulation," Phys. Rev. B **71**, 241102 (2005).

[16] A. N. Norris and H. A. Luo, "Acoustic radiation and reflection from a periodically perforated rigid solid," J. Acoust. Soc. Am. **82**, 2113–2122 (1987).

[17] G. Gonzalez, *Microwave Transistor Amplifiers: Analysis and Design*, 2nd ed. (Prentice-Hall, Englewood Cliffs, 1997).

[18] L. Zhou, Electromagnetic and Acoustic Propagation in Strip Lines and Porous Media Ph.D. thesis, New Jersy Inst. of Technology (2005).